



## Synthesis and structural assignment of two major metabolites of the LTA4H inhibitor DG-051

Livia A. Enache\*, Jun Zhang, David W. Sullins, Isaac Kennedy, Emmanuel Onua, David E. Zembower, Frank W. Mueller, Jasbir Singh, Alex S. Kiselyov

DeCODE Chemistry, Inc., 2501 Davey Road, Woodridge, IL 60517, USA

### ARTICLE INFO

#### Article history:

Received 28 August 2009  
Revised 24 September 2009  
Accepted 25 September 2009  
Available online 29 September 2009

#### Keywords:

Metabolite  
DG-051  
LTA4H inhibitor

### ABSTRACT

The same two major CYP mediated metabolites of **DG-051** were produced in the presence of rat, dog, monkey and human liver microsomes. Their respective structures were hypothesized based on mass spectrometry data correlated with the parent structure and confirmed by comparison with authentic synthetic samples. The number of regioisomers synthesized as candidates for metabolite M1 was narrowed down using a metabolic study of a selectively deuterated **DG-051** analogue.

© 2009 Elsevier Ltd. All rights reserved.

**DG-051** (Fig. 1) is a first-in-class small molecule inhibitor of leukotriene A4 hydrolase (LTA4H), currently in Phase II clinical development for the prevention of heart attack. LTA4H is a zinc metalloprotease encoded by a gene that deCODE studies have linked to increased risk of heart attack.<sup>1</sup> It is directly involved in the synthesis of the pro-inflammatory molecule leukotriene B4 (LTB4).

Understanding the metabolite(s) formed from a new chemical entity (NCE), especially from a development candidate, is an important requirement of the drug development process. In this Letter we describe the identification and synthesis of two major metabolites of **DG-051** produced by CYP mediated pathway. In vitro evaluation of metabolism of **DG-051** was conducted using rat, dog, monkey, and human liver microsomes, while in vivo metabolism studies were conducted in rat and dog. In all tested species, incubation of **DG-051** for 60 min in the presence of an NADPH-generating system<sup>2</sup> yielded the same two major metabolites, designated as **M1** and **M2**. These were analyzed using a high performance liquid chromatograph interfaced with a Q-trap mass spectrometer.<sup>3</sup> To help elucidate the biotransformation site, molecular ions of both **DG-051** ( $m/z$  390) and metabolites ( $m/z$  406 for either **M1** or **M2**) were further analyzed via multiple reaction monitoring (MRM).<sup>4</sup> The product ion spectrum of **DG-051** served as a template and was compared with that of the metabolites. The fragment ions observed for **DG-051** are shown in Figure 2. The product ion scan for both **M1** and **M2** formed following incubation with rat

liver microsome (RLM) gave  $m/z$  406, 16 amu higher than that of the parent **DG-051** ( $m/z$  390). A prominent fragment ion observed from either **M1** or **M2**,  $m/z$  320, was absent from the **DG-051** product ion spectrum [ $m/z$  390→170 (major)→84 or 390→304 (minor)→84] and 16 amu higher than the  $m/z$  304 **DG-051** fragment. This disparity, consistent with addition of an oxygen atom to the  $m/z$  304 ion in Figure 2, was attributed to either hydroxylation of an aromatic ring or N-oxidation of the pyrrolidine moiety.

Interestingly, the fragmentation pathway of **M1** showed 406→320→84, whereas the **M2** pathway also showed 320→302.

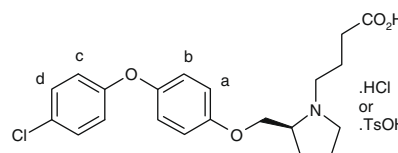


Figure 1. **DG-051** (HCl salt) or **DG-051B** (TsOH salt).

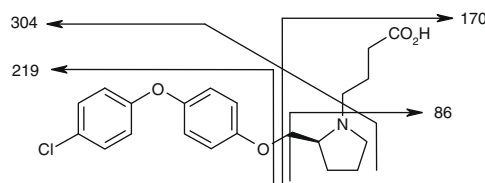


Figure 2. Fragment ions derived from **DG-051**.

\* Corresponding author. Tel.: +1 630 783 4697; fax: +1 630 783 4689.  
E-mail address: [lenache@decode.com](mailto:lenache@decode.com) (L.A. Enache).

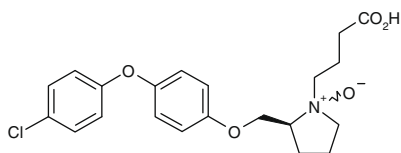


Figure 3. Chemical structure of **DG-051** N-oxide (metabolite **M2**).

The latter pathway suggested loss of a water molecule and supported the idea of the N-oxide as the **M2** metabolite. Gratifyingly, comparison of the LC/MS data for **M2** with that of an available sample of the respective synthetic N-oxide derivative of **DG-051** (Fig. 3) provided a positive match. Notably, under liquid chromatography, the synthetic sample of **DG-051** N-oxide gave two peaks in 9:1 ratio, corresponding to a mixture of two diastereomers. The major peak (diastereomer) co-eluted with the **M2** peak of the microsomal incubation sample. The absolute configuration of **M2** at the N-oxide center has not yet been established.

The identification of **M1**, a phenolic metabolite, was less straightforward. This was due to the relatively close estimated reactivity of the four potential metabolic sites in the diaryl ether pharmacophore (a–d, Fig. 1). To unambiguously determine the **M1** structure, one possible strategy was to synthesize all four possible phenolic derivatives of **DG-051** and compare these synthetic molecules with a metabolized specimen. However, both synthetic involvement and availability of starting materials for this endeavor prompted us to design an alternative approach. In order to narrow down potential metabolic site(s), we prepared a  $D_4$  **DG-051** analogue featuring exhaustive replacement of hydrogens with deuterium atoms within a single aromatic ring (Scheme 1).<sup>5,6</sup>

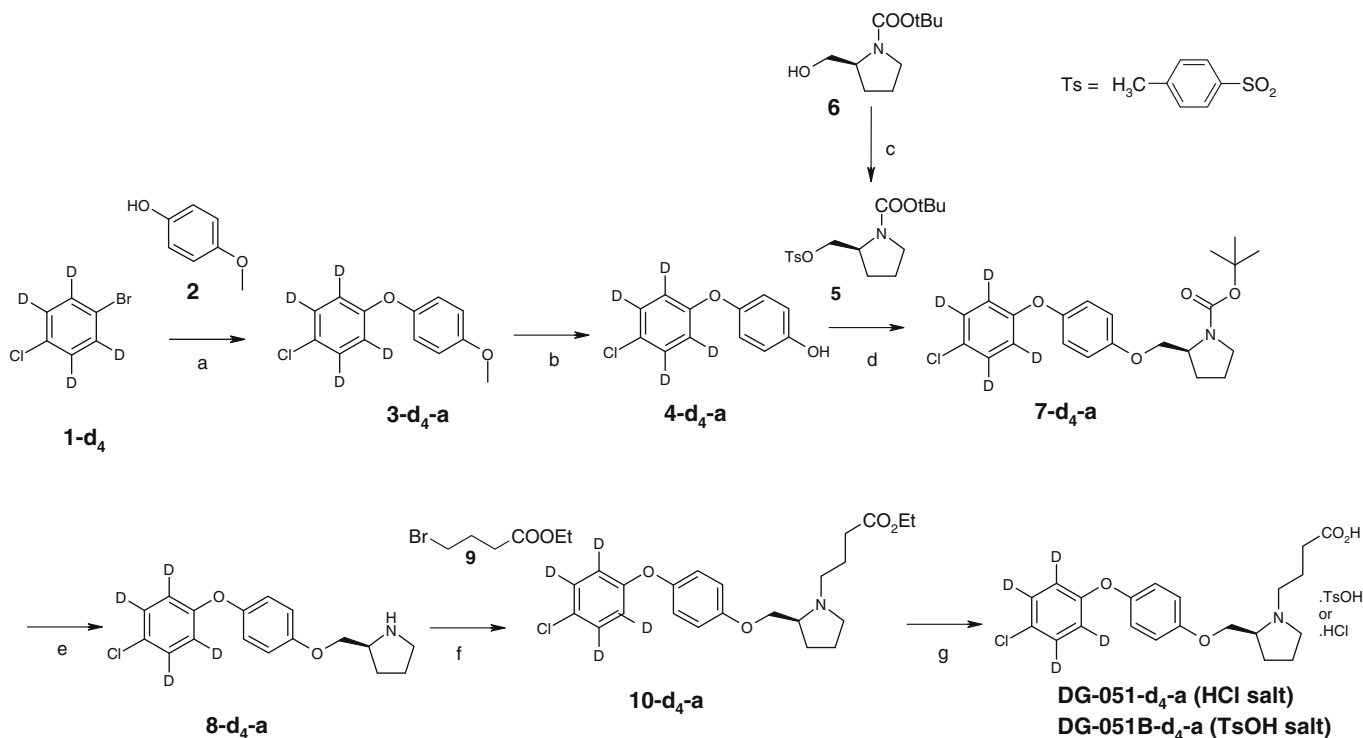
The Ullmann type condensation<sup>7</sup> of commercially available 1-bromo-4-chlorobenzene- $d_4$  (**1-d<sub>4</sub>**) with 4-methoxyphenol **2** provided the diphenyl ether derivative **3-d<sub>4</sub>-a** which was de-methyl-

ated using the trimethylsilyl chloride/sodium iodide protocol.<sup>8</sup> Reaction of the phenoxide derived from phenol **4-d<sub>4</sub>-a** with tosylate **5** (easily accessible from commercially available *tert*-butyl (2S)-2-(hydroxymethyl)pyrrolidine-1-carboxylate **6**) produced key intermediate **7-d<sub>4</sub>-a**. De-protection of the pyrrolidine nitrogen, N-alkylation with ethyl 4-bromobutyrate, saponification, and acidification resulted in the desired tetradeuterated analogue **DG-051-d<sub>4</sub>-a** (**Scheme 1**).

Both **DG-051** and **DG-051-d<sub>4</sub>-a** were subjected to RLM incubation, with and without the addition of NADPH-generating system. The analysis of the reaction product by LC/MS/MS indicated that the **M1** metabolite, while absent in the mixtures lacking NADPH or in the mixtures quenched at 0 min incubation, was present in the RLM mixtures after 60 min incubation, confirming its formation from the CYP mediated metabolic process. The analysis of RLM incubated **DG-051** showed a molecular ion of **M1** at  $m/z$  406. The analysis of RLM incubated **DG-051-d<sub>4</sub>-a** showed a molecular ion of **M1** at  $m/z$  409, indicating that **M1** was a derivative resulting from hydroxylation at the deuterated/halogenated ring (a molecular ion for **M1** of  $m/z$  410 was expected from the same deuterated substrate if the attack had occurred in the non-deuterated ring). This prompted us to conclude that positions 'c' and 'd' (Fig. 1) are likely metabolic sites for **DG-051** to form **M1**.

The corresponding possible metabolite structures were designated M1-A and M1-B (Fig. 4). Both M1-A and M1-B were synthesized as *p*-toluenesulfonate (tosylate) salts, generally easier to isolate than their hydrochloride counterparts or the respective zwitterion forms. The preparation of M1-A is illustrated in Scheme 2.

We had previously prepared intermediate **12** via the reaction of tosylate **5** derived from *N*-Boc-(*S*)-prolinol **6** (Scheme 1) with the phenolate of 4-iodophenol **11**. An Ullmann reaction between the iodobenzene derivative **12** and 4-chloro-2-methoxyphenol **13** produced the key intermediate **14** which was de-protected and N-alkylated with ethyl 4-bromobutyrate. The selective de-methyl-



Scheme 1. Reagents and conditions: (a) CuI, *N,N*-dimethylglycine-HCl, Cs<sub>2</sub>CO<sub>3</sub>, 1,4-dioxane, 110 °C, 1.5 h; (b) TMSCl, NaI, acetonitrile, reflux 20 h; (c) TsCl, TEA, DMAP, DCM, rt, 16 h, 97%; (d) KO<sup>t</sup>Bu, DMF, 55 °C, 16 h, 61% (three steps); (e) 4 M HCl in 1,4-dioxane, rt, 16 h, 79%; (f) K<sub>2</sub>CO<sub>3</sub>, acetonitrile, 50 °C, 16 h; (g) NaOH, EtOH, H<sub>2</sub>O, rt, 16 h, then HCl or TsOH·H<sub>2</sub>O, 80–90% (two steps).

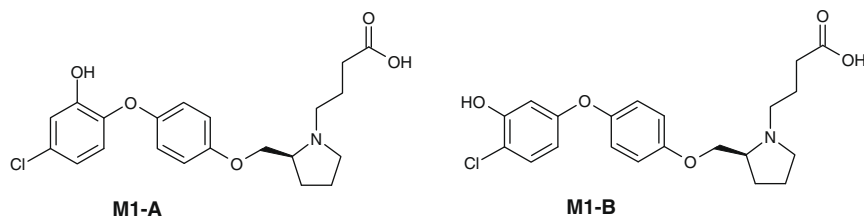
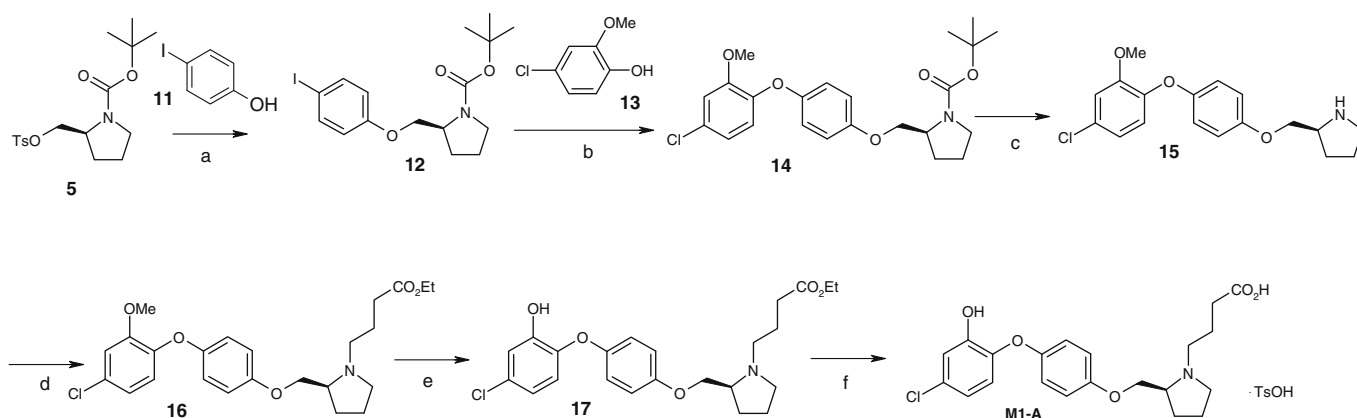


Figure 4. Proposed structures of the M1 metabolite of DG-051.

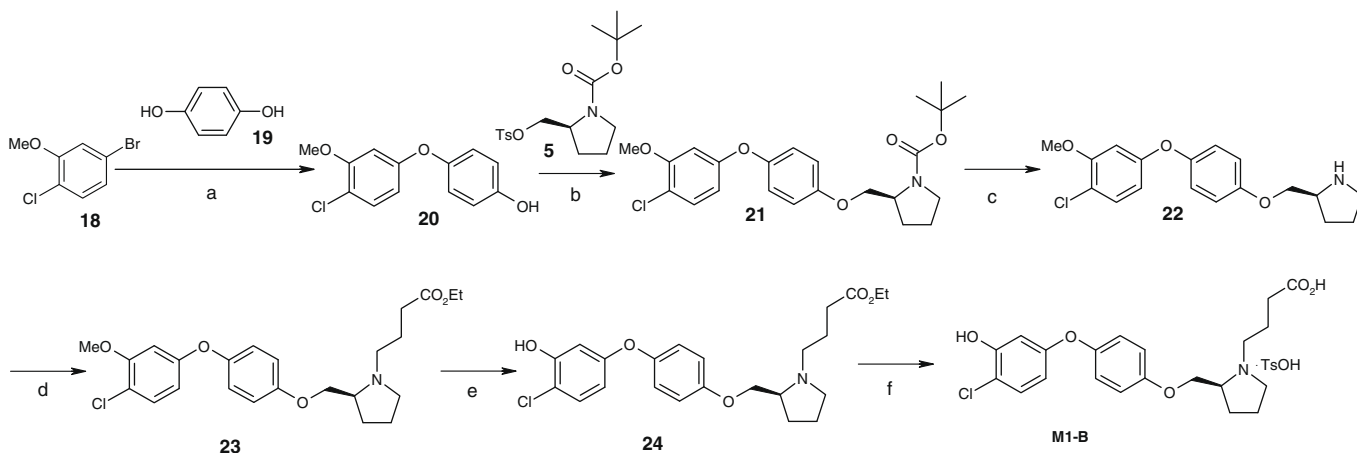


Scheme 2. Reagents and conditions: (a) KO<sup>t</sup>Bu, DMF, 45–55 °C, 20 h, 92%; (b) CuI, *N,N*-dimethylglycine·HCl, Cs<sub>2</sub>CO<sub>3</sub>, 1,4-dioxane, 95 °C, 22 h, 54%; (c) 4 M HCl in 1,4-dioxane, rt, 2 h; (d) ethyl 4-bromobutyrate, K<sub>2</sub>CO<sub>3</sub>, acetonitrile, 60 °C, 16 h; (e) NaSEt, DMF, 95 °C, 1 h, 67% (three steps); (f) NaOH, EtOH, H<sub>2</sub>O, rt, 16 h, then TsOH·H<sub>2</sub>O, 79%.

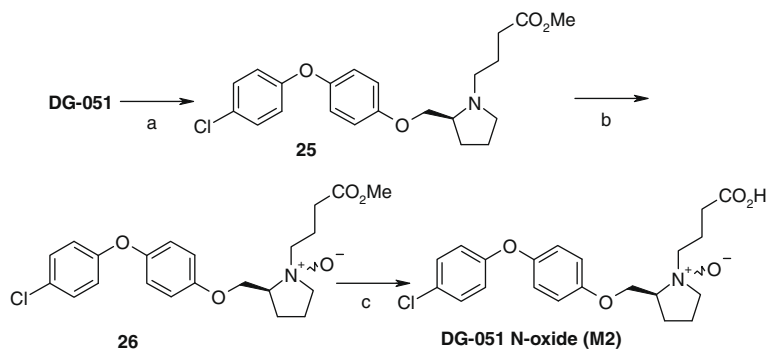
ation of intermediate **16** in the presence of the ester and the other ether functionalities was not trivial. Boron tribromide in dichloromethane (DCM) afforded a complex product mixture. A complex mixture was also obtained when using the TMSCl/NaI procedure in similar fashion to its application per Scheme 1. Heating **16** with a small excess of sodium ethanethiolate (1.6 equiv) in dimethylformamide (DMF) at 95 °C for 1–3 h provided the desired intermediate **17** after concentration and aqueous work-up. An early pilot showed very low recovery (29%). We attributed this to partial hydrolysis of the ester functionality during a longer reaction time (3 h) and subsequent loss of the free acid in the aqueous wash. In a later installment, we both confirmed this hypothesis and solved the low recovery issue by stopping the reaction after only 1 h (at which point TLC on silica gel with 1:9 (v/v) MeOH/DCM showed a much less intense free acid spot at the baseline than in

the early experiment) and by refluxing the crude isolated product in excess EtOH in the presence of catalytic amounts of hydrochloric acid (to re-esterify the free acid traces). The de-methylated intermediate **17** was thus isolated in 67% yield over three steps, after chromatographic separation. Saponification and tosylate salt formation completed the synthesis of **M1-A**.<sup>9</sup>

Preparation of **M1-B** (Scheme 3) started with the Ullmann reaction between 5-bromo-2-chloroanisole **18** and hydroquinone **19**. A relatively large excess (6 equiv) of hydroquinone was required to achieve a satisfactory conversion rate. The product (**20**) was contaminated with a significant amount of *p*-benzoquinone and was used in the next step without further purification. The *O*-alkylation of the phenolate derived from **20** with tosylate **5** (prepared as in Scheme 1) produced the key intermediate **21** in a 14–21% yield for the two step sequence including chromatography. Cleavage of



Scheme 3. Reagents and conditions: (a) CuI, *N,N*-dimethylglycine·HCl, Cs<sub>2</sub>CO<sub>3</sub>, 1,4-dioxane, 95 °C, 70 h; (b) KO<sup>t</sup>Bu, DMF, 55 °C, 48 h, 14–21% (two steps); (c) 4 M HCl in 1,4-dioxane, rt, 16 h, 51%; (d) ethyl 4-bromobutyrate, K<sub>2</sub>CO<sub>3</sub>, acetonitrile, 55 °C, 16 h, 85%; (e) NaSEt, DMF, 95 °C, 1 h; (f) NaOH, EtOH, H<sub>2</sub>O, rt, 16 h, then TsOH·H<sub>2</sub>O, 32% (two steps).



**Scheme 4.** Reagents and conditions: (a) MeOH, 4 M HCl in 1,4-dioxane, reflux, 4 h, then Na<sub>2</sub>CO<sub>3</sub>, 100%; (b) MCPBA, DCM, –78 °C to rt, 16 h, 79%; (c) aq NaOH, rt, 16 h, then HCl to pH 3.7–3.9, 99%.

the carbamate, alkylation, de-methylation, and saponification were conducted similar to the protocol for the synthesis of **M1-A** to afford **M1-B**.<sup>10</sup>

Finally, the N-oxide derivative of **DG-051**, previously identified as the **M2** metabolite, was re-synthesized via the route summarized in Scheme 4.

Notably, **DG-051** can be directly N-oxidized with 3-chloroperbenzoic acid (MCPBA) or other oxidizing agents. However, the resulting N-oxide was not stable on silica gel. It was not amenable to re-crystallization due to both its glassy consistency and its low melting point. In our hands, the more practical approach to high purity N-oxide involved preparation of the **DG-051** methyl ester as a free base (**25**). Ester **25** was subsequently N-oxidized to generate intermediate **26** in reasonable yield (79%) after chromatographic purification. Saponification of **26** followed by careful acidification to mildly acidic pH and extraction work afforded 99.5% pure **DG-051** N-oxide.<sup>11</sup>

HPLC traces for **M1-A**, **M1-B**, and **M2** were compared to that of the authentic metabolite mixture formed during the incubation of

**DG-051** with dog liver microsomes (DLM) (Fig. 5). We re-confirmed the N-oxide to be the **M2** metabolite and identified the structure of **M1** to be **M1-A**. Both **M1** and **M2** exhibited an increase in abundance that was dependent on the incubation time.

Structure **M1-A**, hydroxylated at position 'c' (Fig. 1), is consistent with the most favorable position for CYP mediated metabolic attack resulting (albeit based on only ca. 1 kcal/mol energy difference) from computational analysis that took into account (i) hydrogen abstraction energy (lowest value desired) and (ii) Connolly surface area used as surrogate for solvent accessible surface area (SASA) (highest value desired).<sup>12a</sup> The respective calculated values (hydrogen abstraction energy in kcal/mol/Connolly surface area in Å<sup>2</sup>) for positions a–d in Figure 1 are (a) –56.59/7.65; (b) –60.00/7.25; (c) –61.16/7.61; and (d) –58.17/6.89. All the absolute values of the calculated hydrogen abstraction energies appear high relative to average calculated values available in literature,<sup>12c</sup> while the calculated Connolly surface areas are all below 8 Å<sup>2</sup>. Due to these considerations and to the fact that these types of calculations generally have a lower level of prediction capability for hydroxylation at the sp<sup>2</sup> carbon,<sup>12b,c</sup> we did

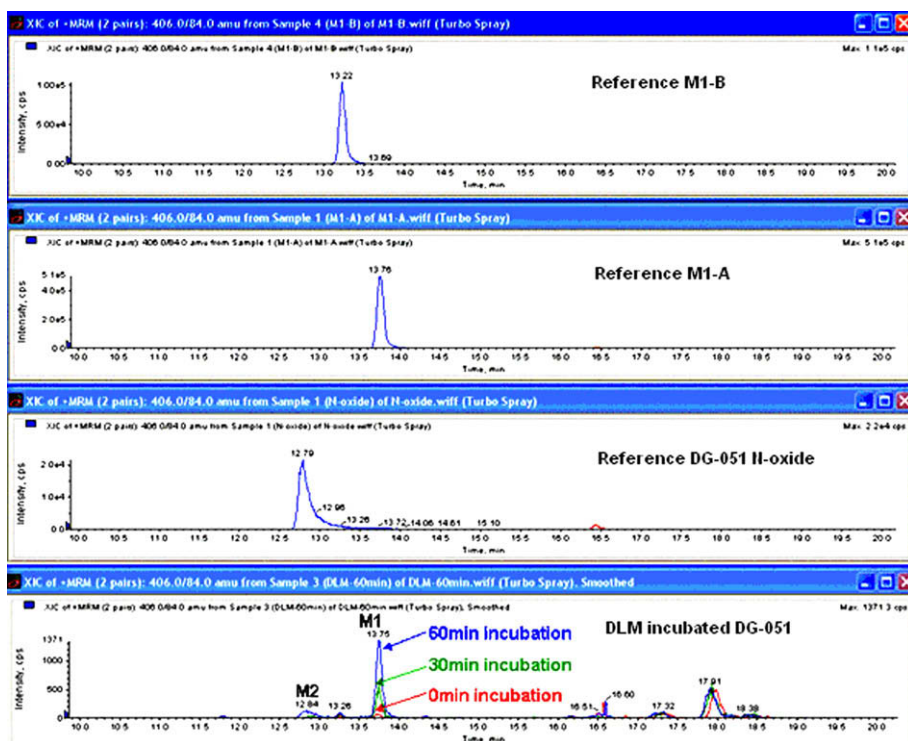


**Figure 5.** HPLC comparison of authentic standards with metabolites **M1** and **M2** from DLM incubated **DG-051**.

not use the calculated results as a definitive tool at the structural assignment stage. However, we find it useful to mention them for comparison with the experimental findings. Furthermore, position 'c' as the preferred site of CYP mediated attack also matches our latest computational results obtained with a mechanism based approach. The respective calculated values (activation energy/reaction enthalpy, both in kcal/mol) for sites a–d in Figure 1 are (a) –31.11/–39.95; (b) –33.95/–42.52; (c) –34.54/–50.53; and (d) –32.46/–33.79.<sup>13a,b</sup>

In conclusion, we have successfully identified two key CYP mediated metabolites for the Phase II clinical candidate **DG-051**. The evaluation sequence for **M1** involved preparation of the tetradeuterated molecule **DG-051-d<sub>4</sub>-a**. Studies revealed two possible aromatic sites for metabolic hydroxylation. The specific reactive center was further identified by comparison of the metabolized mixture with authentic synthetic samples of the two possible candidate structures, each prepared via a six step synthetic sequence. Positive identification of **M2** was achieved by a tandem MSMS analysis of the metabolite peak followed by chemical synthesis and comparison with the metabolized sample.

### Acknowledgment

The authors gratefully acknowledge computational chemistry contributions from Dr. Rama K. Mishra.

### References and notes

- Sandanayaka, V.; Mamat, B.; Mishra, R. K.; Winger, J.; Krohn, M.; Zhao, L.-M.; Keyvan, M.; Enache, L. A.; Sullins, D.; Onua, O.; Zhang, J.; Halldorsdottir, G.; Sigthorsdottir, H.; Thorlaksdottir, A.; Sigthorsson, G.; Thorsteinnsson, M.; Davies, D. R.; Stewart, L. J.; Zembower, D. E.; Andresson, T.; Kiselyov, A. S.; Singh, J.; Gurney, M. E. *J. Med. Chem.*, submitted for publication.
- Liver microsomes (from Xenotech LLC, Lenexa, KS) were incubated with **DG-051** in a system consisting of microsomes and NADPH-generating system (containing  $\text{KH}_2\text{PO}_4$ ,  $\text{K}_2\text{HPO}_4$ ,  $\text{MgCl}_2$ , EDTA, and deionized water). For incubation, the diluted microsomes were mixed with **DG-051** (1000  $\mu\text{L}$  of microsomes and 200  $\mu\text{L}$  of **DG-051**) in glass vials, and pre-incubated for 10 min at 37 °C. The reaction was initiated by the addition of 1000  $\mu\text{L}$  of the NADPH-generating system, and the capped glass vials were set in a shaking incubator at 37 °C for up to 60 min. Samples were removed at 0 min (baseline) and at appropriate intervals in order to track the formation of each metabolite and the concomitant disappearance of the parent compound. At each sampling time, 200  $\mu\text{L}$  of incubation mixture was removed and mixed with 200  $\mu\text{L}$  ice-cold acetonitrile. The samples were vortexed to mix for approximately 1 min, and centrifuged at 3000g for 30 min. The supernatant was transferred into clean plates, and analyzed using appropriate LC/MS/MS methods. Final incubation mixture contained 1.8 mg/mL microsomal protein and 25  $\mu\text{M}$  **DG-051** per reaction well.
- LC/MS/MS was performed using a Finnigan LCQ spectrometer with ion trap analyzer from Thermo Scientific.
- (a) Kondrat, R. W.; McClusky, G. A.; Cooks, R. G. *Anal. Chem.* **1978**, *50*, 2017; (b) Yu, X.; Cui, D.-H.; Davis, M. R. *J. Am. Soc. Mass Spectrom.* **1999**, *10*, 175; (c) Lim, H. K.; Stellingweif, S.; Sisenwine, S.; Chan, K. W. *J. Chromatogr.* **1999**, *831*, 227; (d) Anderson, L.; Hunter, C. L. *Mol. Cell. Proteomics* **2006**, *5*, 573.
- When following the same route towards the preparation of the analogue **DG-051-d<sub>4</sub>-b** (tetradeuterated at the two 'a' positions and the two 'b' positions from Fig. 4) starting from 1-bromo-4-chlorobenzene (**1**) and 4-methoxyphenol-*d*<sub>4</sub> (**2-d<sub>4</sub>**), we noticed that the resulting product was contaminated with analogues having a lower level of labeling (*d*<sub>3</sub>, *d*<sub>2</sub>). Most likely, deuterium to hydrogen exchange had occurred under the conditions of the first step, via quino-phenolic tautomerism of **2-d<sub>4</sub>**.
- There were no differences between the metabolite patterns of the hydrochloride salt, **DG-051-d<sub>4</sub>-a** and the tosylate salt, **DG-051B-d<sub>4</sub>-a**.
- Ma, D.; Cai, Q. *Org. Lett.* **2003**, *5*, 3799.
- Olah, G. A.; Narang, S. C.; Gupta, B. G. B.; Malhotra, R. *J. Org. Chem.* **1979**, *44*, 1247.
- Spectral data for **M1-A** (TsOH salt): <sup>1</sup>H NMR (400 MHz, DMSO-*d*<sub>6</sub>)  $\delta$  1.82 (m, 1H), 1.85–2.19 (m, 4H), 2.21 (m, 1H), 2.29 (s, 3H), 2.36 (t, *J* = 7.2 Hz, 2H), 3.14 (m, 2H), 3.42 (m, 1H), 3.57 (m, 1H), 3.88 (m, 1H), 4.10 (dd, *J* = 10.8, 8.0 Hz, 1H), 4.26 (dd, *J* = 10.8, 3.6 Hz, 1H), 6.83 (dd, *J* = 8.8, 2.0 Hz, 1H), 6.86 (d, *J* = 8.8 Hz, 1H), 6.88 (d, *J* = 9.2 Hz, 2H), 6.97 (d, *J* = 9.2 Hz, 2H), 6.98 (d, *J* = 2.0 Hz, 1H), 7.11 (d, *J* = 8.0 Hz, 2H), 7.48 (d, *J* = 8.0 Hz, 2H), 8.80 (br s, 1H), 10.02 (s, 1H), 12.00 (br s, 1H) ppm; <sup>13</sup>C NMR (500 MHz, DMSO-*d*<sub>6</sub>)  $\delta$  20.73, 20.76, 22.40, 26.21, 30.47, 54.24 (2 signals), 65.90, 67.00, 115.63, 116.82, 118.07, 119.16, 121.72, 125.45, 127.85, 128.00, 137.52, 143.08, 145.76, 149.88, 151.52, 153.09, 173.58 ppm; MS (APCI+) *m/z* 406 [MH<sup>+</sup>].
- Spectral data for **M1-B** (TsOH salt): <sup>1</sup>H NMR (500 MHz, DMSO-*d*<sub>6</sub>)  $\delta$  1.83 (m, 1H), 1.87–2.12 (m, 4H), 2.24 (m, 1H), 2.29 (s, 3H), 2.38 (t, *J* = 7.0 Hz, 2H), 3.18 (m, 2H), 3.48 (m, 1H), 3.63 (m, 1H), 3.93 (m, 1H), 4.14 (dd, *J* = 10.5, 8.5 Hz, 1H), 4.31 (dd, *J* = 10.5, 3.5 Hz, 1H), 6.35 (dd, *J* = 9.0, 3.0 Hz, 1H), 6.54 (d, *J* = 3.0 Hz, 1H), 7.05 (s, 4H), 7.11 (d, *J* = 8.0 Hz, 2H), 7.27 (d, *J* = 9.0 Hz, 1H), 7.47 (d, *J* = 8.0 Hz, 2H), 9.44 (br s, 1H), 10.28 (s, 1H), 12.32 (br s, 1H) ppm; <sup>13</sup>C NMR (500 MHz, DMSO-*d*<sub>6</sub>)  $\delta$  20.58, 20.72, 22.37, 26.15, 30.38, 54.36, 54.40, 66.22, 66.80, 105.59, 108.81, 113.48, 115.88, 120.92, 125.44, 127.96, 130.33, 137.46, 145.83, 149.71, 153.94, 154.07, 157.52, 173.52 ppm; MS (APCI-) *m/z* 404 [M–1].
- Spectral data for **DG-051 N-oxide**: <sup>1</sup>H NMR (400 MHz, CDCl<sub>3</sub>)  $\delta$  2.00–2.18 (m, 3H), 2.18–2.45 (m, 4H), 2.52 (m, 1H), 3.68 (m, 2H), 4.00–4.14 (m, 3H), 4.19 (m, 1H), 4.70 (dd, *J* = 11.6, 8.0 Hz, 1H), 6.85 (d, *J* = 8.8 Hz, 2H), 6.88 (d, *J* = 9.2 Hz, 2H), 6.94 (d, *J* = 9.2 Hz, 2H), 7.24 (d, *J* = 8.8 Hz, 2H) ppm; <sup>13</sup>C NMR (500 MHz, CDCl<sub>3</sub>)  $\delta$  19.58, 20.28, 25.04, 32.54, 64.76, 65.13, 65.80, 75.60, 115.86, 118.91, 120.77, 127.55, 129.56, 150.64, 154.00, 156.77, 175.96 ppm; MS (APCI-) *m/z* 404 [M–1].
- (a) We used the Austin model-1 (AM1) Hamiltonian to calculate the hydrogen abstraction energy. The Connolly surface area was calculated using the MOLCAD module of SYBYL7.0; (b) Singh, S. B.; Shen, L. Q.; Walker, M. J.; Sheridan, R. P. *J. Med. Chem.* **2003**, *46*, 1330; (c) Sheridan, R. P.; Korzekwa, K. R.; Torres, R. A.; Walker, M. J. *J. Med. Chem.* **2007**, *50*, 3173.
- (a) Jones, J. P.; Mysinger, M.; Korzekwa, K. R. *Drug Metab. Dispos.* **2002**, *30*, 7; (b) Methoxy radical was added to the different positions of the aromatic rings. The heat of reaction and the transition state were computed for each reaction using the AM1 formalism.